

# **Integrating hollow spherical covalent organic framework on NH<sub>2</sub>-MIL-101(Fe) as high performance heterogeneous photocatalysts**

Yuqi Wan, ‡<sup>a</sup> Huaizhi Yang, ‡<sup>a</sup> Qigao Shang, <sup>a,b</sup> Qingrong Cheng, <sup>a,\*</sup> Hong Zhou, <sup>a</sup> Zhiquan Pan<sup>a</sup>

<sup>a</sup> School of Chemistry and Environmental Engineering, Wuhan Institute of Technology, Wuhan, 430205, PR China.

<sup>b</sup> Faculty of Materials Science and Chemistry, China University of Geosciences, Wuhan, 430074, PR China.

Corresponding authors:

\*(Q.C.) E-mail: [chengqr383121@sina.com](mailto:chengqr383121@sina.com)

‡These authors contributed equally to this work.

**Total number of pages: 8**

**Total number of Tables: 2**

**Total number of Figures: 10**

**Physical Measurements**

The morphologies and microstructural information of the samples were characterized by scanning electron microscopy (SEM, Gemini 500). The elementary composition was acquired by an F20 field-emission gun equipped with an energy-dispersive X-ray spectrometer (EDS). All composites were investigated in air through powder X-ray diffraction measurements (PXRD, Bruker D8-Advance X-ray diffractometer with Cu K $\alpha$  radiation,  $\lambda = 1.5418 \text{ \AA}$ ), from  $5^\circ$  to  $90^\circ$  with a scanning rate of  $5^\circ \text{ min}^{-1}$  at room temperature. The ultraviolet-visible (UV-vis) diffuse reflectance spectra (DRS) were measured on a SHIMADZU UV-2600 spectroscope equipped with an integrating sphere assembly and using BaSO $_4$  as the reference. X-ray photoelectron spectroscopy (XPS) was performed by using a Thermo ESCALAB 250Xi-XPS photoelectron spectrometer with an Al K $\alpha$  X-ray resource. The shift of the binding energy was referenced to the C 1s level at 284.8 eV as an internal standard. Thermogravimetric analyses were conducted on a Pyris Diamond TG (Perkin Elmer) apparatus at a heating rate of  $10 \text{ K min}^{-1}$  from  $30^\circ \text{C}$  to  $900^\circ \text{C}$  under nitrogen flow.

### **Photocatalytic degradation experiments**

The photocatalytic activities of the NH $_2$ -MIL-101(Fe)@SNW-1 heterojunction were evaluated via the photocatalytic degradation of three different kinds of pollutants, such as ciprofloxacin (CIP), tetracycline hydrochloride (TC) and rhodamine B (RhB) in aqueous solution under visible light irradiation. A 300 W Xe lamp provided sunlight irradiation. Aqueous solutions of CIP (100 mL,  $10 \text{ mgL}^{-1}$ ), TC (100 mL,  $20 \text{ mgL}^{-1}$ ) and RhB (100 mL,  $20 \text{ mgL}^{-1}$ ) were added in the different Pyrex photocatalytic reactors. In each experiment, 30 mg of photocatalyst was added into the pollutant solution. Prior to irradiation, the suspensions were magnetically stirred in the dark for 30 min to achieve absorption-desorption equilibrium between the photocatalyst and pollutants. At certain time intervals, 3 mL suspensions were sampled and centrifuged ( $16000 \text{ rpm}$ , 3 min) to remove the photocatalyst particles. The concentrations of CIP, TC and RhB were monitored using an UV-vis spectrophotometer (UV-2450, Shimadzu) according to its absorbance at 276 nm, 356 nm and 553 nm respectively. The durability tests of NH $_2$ -MIL-101(Fe)@SNW-1 catalyst were carried out by using the same procedure as above and the product underwent four consecutive cycles, each lasting for 300~360 min. After each cycle, the catalyst was centrifuged, washed thoroughly with deionized water, and then added to fresh CIP, TC and RhB solutions.

In order to confirm the reproducibility of the results, the degradation experiments were carried out with duplicated runs for each condition, and the experimental error was calculated to be within  $\pm 5\%$ .

### Photocatalytic hydrogen evolution

Photocatalytic hydrogen evolution was conducted in a 150 mL cylindrical quartz reactor. The light source was a 300 W xenon lamp (Perfect Light, PLS-SXE300C, Beijing). 50 mg photocatalysts was dispersed 100 mL DI water with 15 mL TEOA as sacrifice agent were mixed. And  $\text{H}_2\text{PtCl}_6$  was used as the precursor of the Pt species to photo-deposit on the photocatalysts. Before light irradiation, the air in the reactor was removed by nitrogen to keep the reaction anaerobic. 300  $\mu\text{L}$  of gas was extracted by injection needle from the reactor each hour. The rate of Photocatalytic hydrogen evolution was calculated by gas chromatography (Tianmei GC 7900, TCD,  $\text{N}_2$  as a carrier) using the standard curve. Photocatalytic cycle experiment was operated as follows: after the first photocatalytic reaction finished, the photocatalyst was centrifuged into a new solution system to test again under the same conditions. The process was repeated four times.

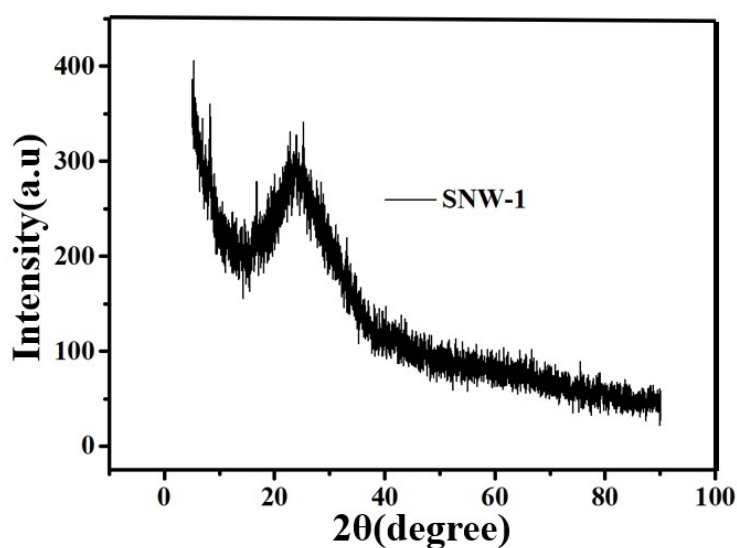
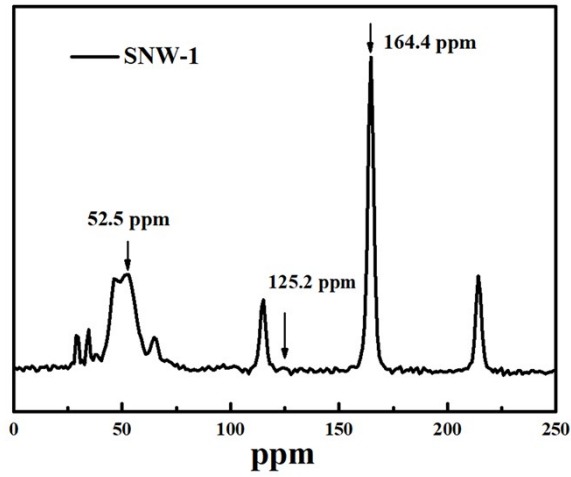
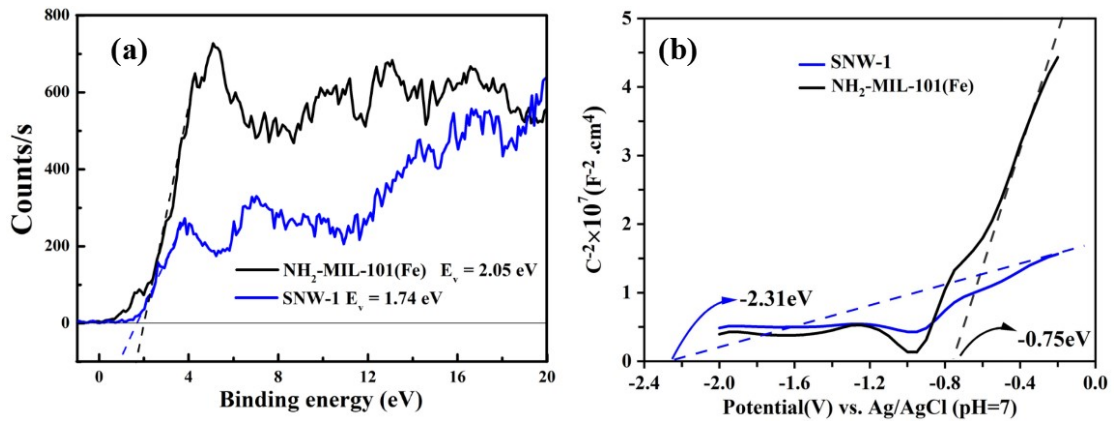


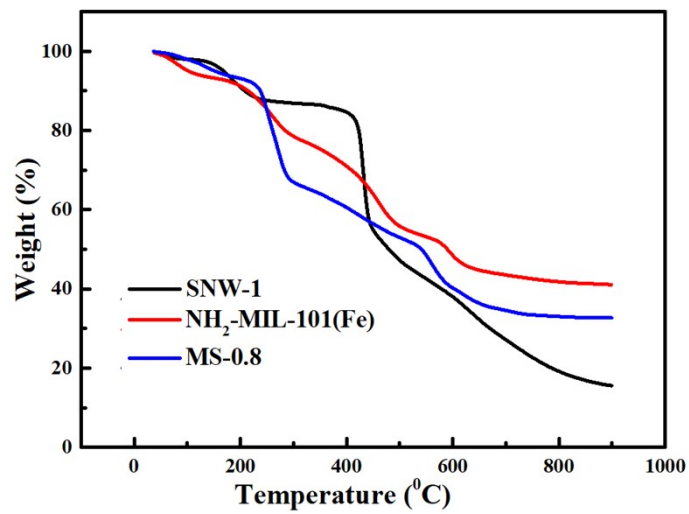
Fig.S1 XRD patterns of the SNW-1



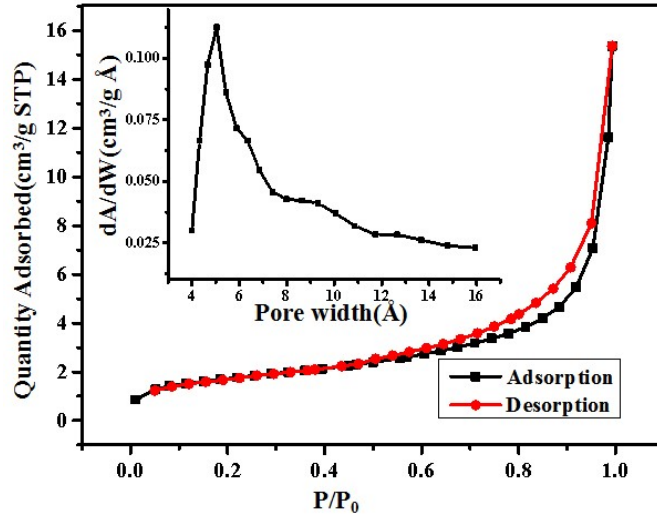
**Fig.S2**  $^{13}\text{C}$  CP/MAS NMR spectrum of SNW-1



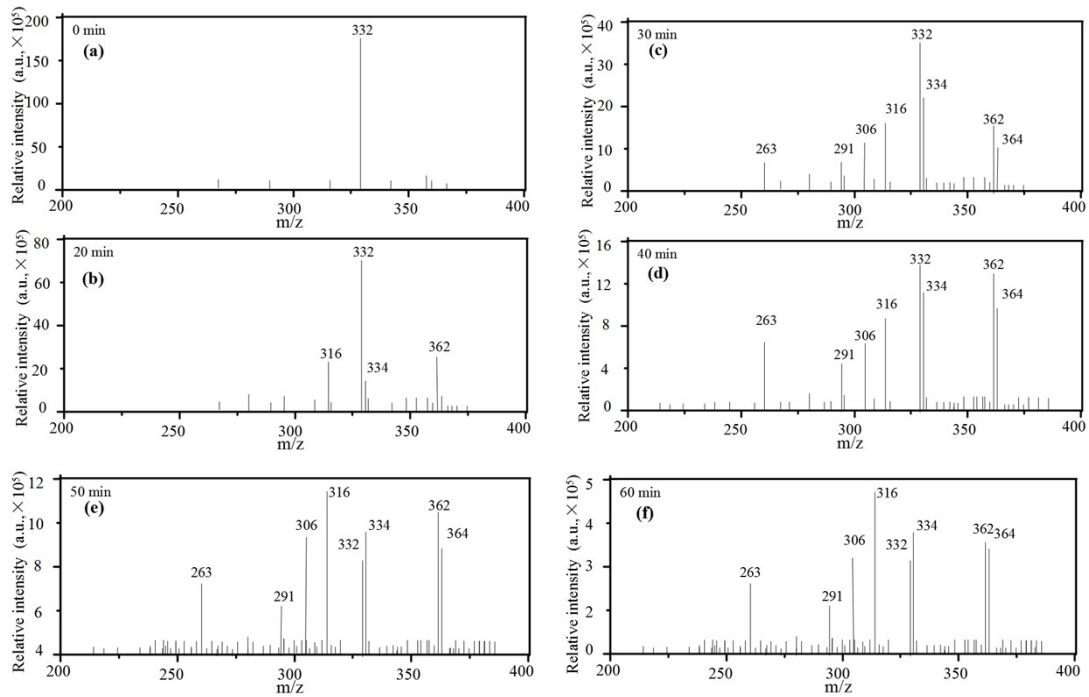
**Fig.S3** (a) The valence band XPS patterns of  $\text{NH}_2\text{-MIL-101(Fe)}$  and SNW-1, (b) Mott-Schottky plots of  $\text{NH}_2\text{-MIL-101(Fe)}$  and SNW-1.



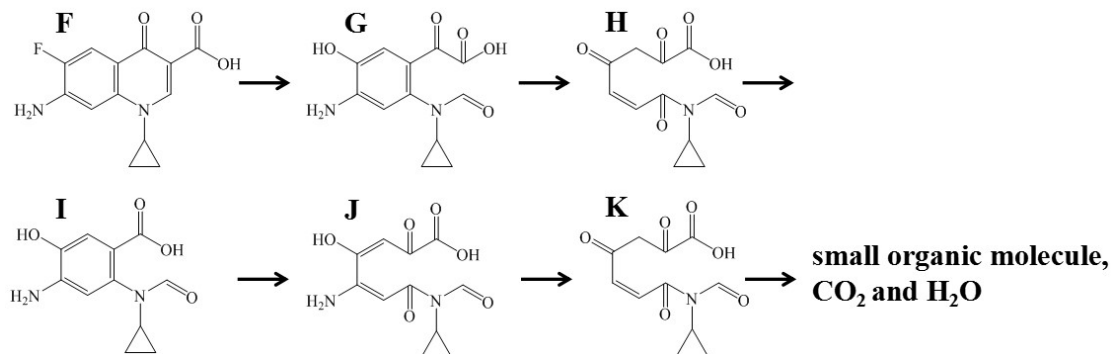
**Fig.S4** TG curves of SNW-1,  $\text{NH}_2\text{-MIL-101(Fe)}$  and SNW-0.8



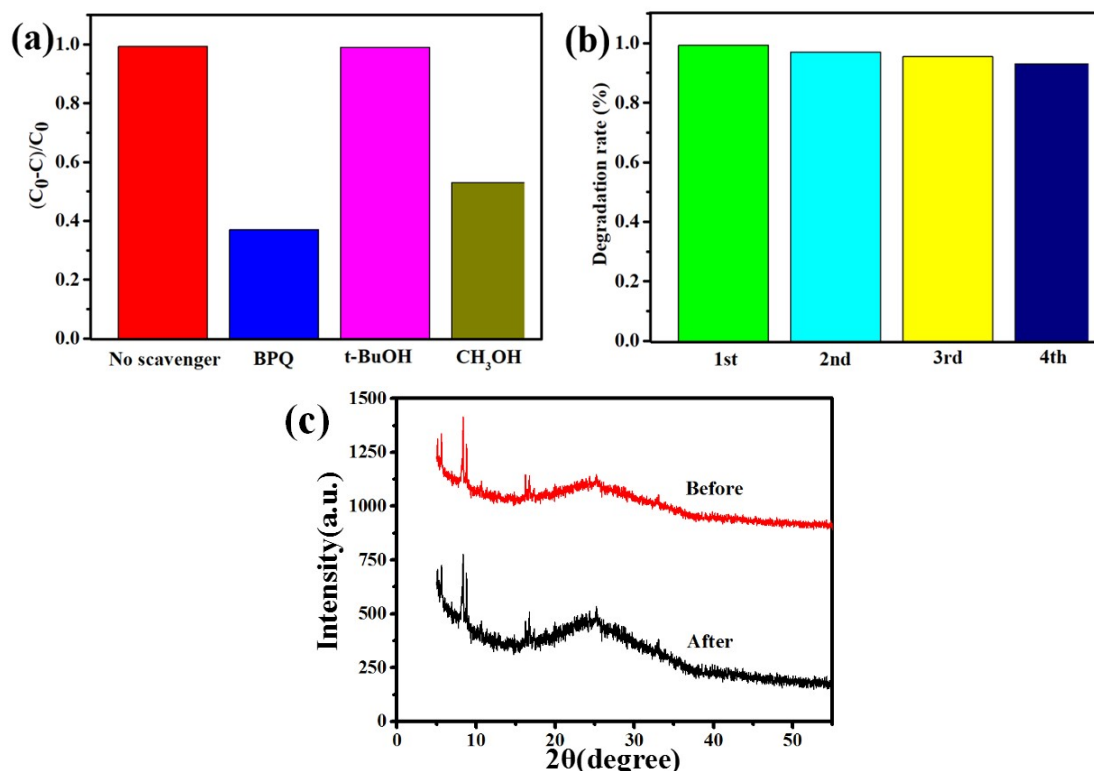
**Fig.S5** N<sub>2</sub> adsorption isotherms of MS-0.8; the pore size distribution graph is given in the inset.



**Fig.S6** The mass spectra of intermediates during ciprofloxacin degradation.



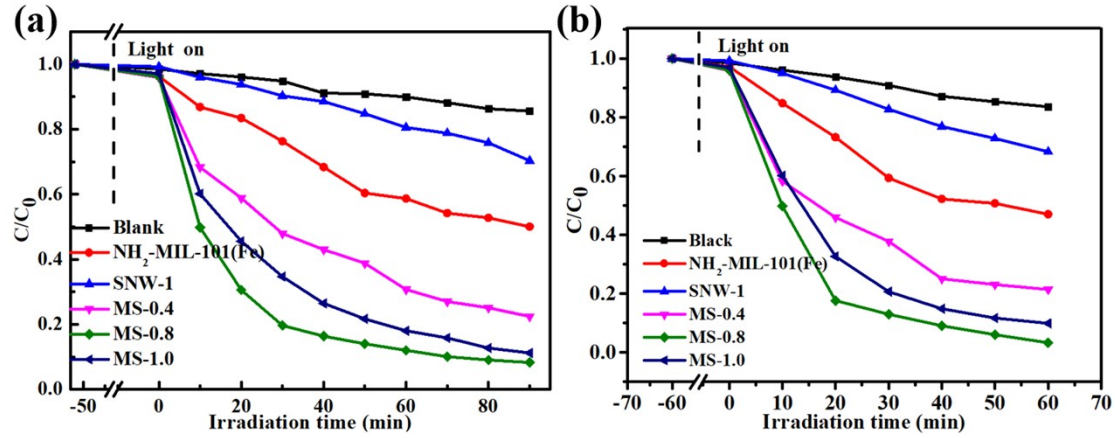
**Fig.S7** The transformation pathways of product F from ciprofloxacin.



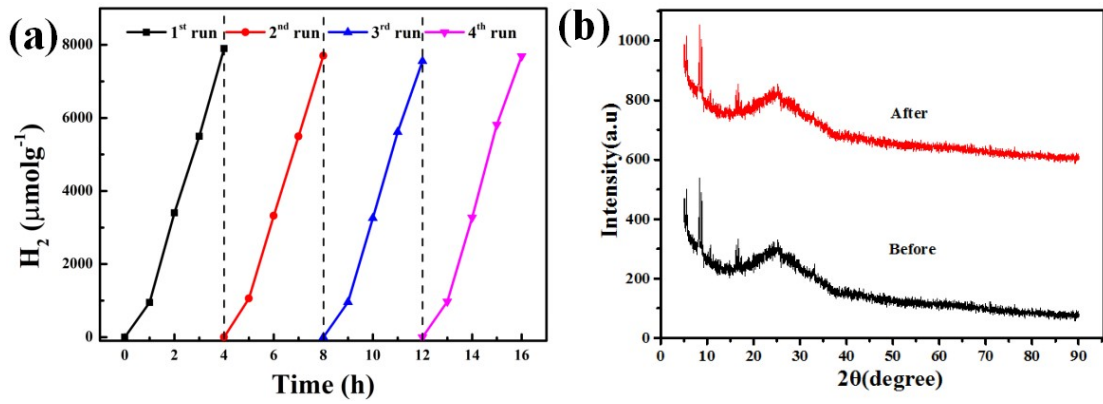
**Fig.S8** The radical trapping test for MS-0.8(a), the recycling performance of MS-0.8 in the photocatalytic degradation of CIP during four continuous times(b). The PXRD patterns for MS-0.8 before and after photocatalytic degradation of CIP(c).

Table S1 A comparison of the photocatalytic CIP degradation over MIL-101(Fe)-based photocatalysts

Photocatalysts /mg	$V$ (mL) / $C_0$ ( $mg \cdot L^{-1}$ )	Excitation source	Time (min)	Result (%)	Ref
SM-0.8/20	100/10	Sun light	60	97.3	This work
CUMSs/MIL-101(Fe, Cu) /H <sub>2</sub> O <sub>2</sub> /10	100/20	3 mM H <sub>2</sub> O <sub>2</sub>	30	93.5	1
MIL-101(Fe,Co)/H <sub>2</sub> O <sub>2</sub> /20	100/20	50 $\mu$ L H <sub>2</sub> O <sub>2</sub>	30	97.8	2
NH <sub>2</sub> -MIL-53(Fe)/AgSCN/20	200/20	visible light 100 $\mu$ L H <sub>2</sub> O <sub>2</sub>	60	90	3



**Fig.S9** Photocatalytic degradation of TC (a) and RhB (b) over different samples.



**Fig.S10** Four cycles of photocatalytic  $\text{H}_2$  production over MS-0.8(a). The PXRD patterns for MS-0.8 before and after photocatalytic hydrogen evolution(b).

**Table S2** Comparison of the photocatalytic  $\text{H}_2$  evolution rates over different photocatalysts.

Photocatalysts /mg	Irrigation	Sacrificial agents	Cocatalysts	Activity $\mu\text{mol}\cdot\text{g}^{-1}\cdot\text{h}^{-1}$	Ref
SM-0.8/50	Sun light	TEOA	Pt	1949.56	This work
$\text{NH}_2\text{-MIL-125(Ti)/B-CTF-1/20}$	vis	TEOA	Pt	360	4
CdS/PI	vis	lactic acid	Pt	613	5
CdS@NU-1000/50	vis	$\text{Na}_2\text{S}$ $\text{Na}_2\text{SO}_3$	Pt	1870	6
UiO-66/CdS/50	vis	$\text{Na}_2\text{S}$ $\text{Na}_2\text{SO}_3$	Pt	1700	7
$\text{N}_3\text{-COF/5}$	vis	TEOA	Pt	1703	8
POM@UiO-66	vis	MeOH	-	699	9
Ti-MOF-Ru(tpy) <sub>2</sub> /10	vis	TEOA	Pt	200	10
CdS/CTNBs/10	vis	TEOA	Pt	730	11

## References

1. F1. H. Liang, R. Liu, X. An, C. Hu, X. Zhang and H. Liu, Bimetal-organic frameworks with coordinatively unsaturated metal sites for highly efficient Fenton-like catalysis, *Chemical Engineering Journal*, 2021, **414**.
2. H. Liang, R. Liu, C. Hu, X. An, X. Zhang, H. Liu and J. Qu, Synergistic effect of dual sites on bimetal-organic frameworks for highly efficient peroxide activation, *J Hazard Mater*, 2021, **406**, 124692.
3. J. Yi, X. Wu, H. Wu, J. Guo, K. Wu and L. Zhang, Facile synthesis of novel NH<sub>2</sub>-MIL-53(Fe)/AgSCN heterojunction composites as a highly efficient photocatalyst for ciprofloxacin degradation and H<sub>2</sub> production under visible-light irradiation, *Reaction Chemistry & Engineering*, 2022, **7**, 84-100.
4. F. Li, D. Wang, Q.-J. Xing, G. Zhou, S.-S. Liu, Y. Li, L.-L. Zheng, P. Ye and J.-P. Zou, Design and syntheses of MOF/COF hybrid materials via postsynthetic covalent modification: An efficient strategy to boost the visible-light-driven photocatalytic performance, *Applied Catalysis B: Environmental*, 2019, **243**, 621-628.
5. Y. Hu, X. Hao, Z. Cui, J. Zhou, S. Chu, Y. Wang and Z. Zou, Enhanced photocarrier separation in conjugated polymer engineered CdS for direct Z-scheme photocatalytic hydrogen evolution, *Applied Catalysis B: Environmental*, 2020, **260**.
6. P. P. Bag, X.-S. Wang, P. Sahoo, J. Xiong and R. Cao, Efficient photocatalytic hydrogen evolution under visible light by ternary composite CdS@NU-1000/RGO, *Catal. Sci. Technol.*, 2017, **7**, 5113-5119.
7. R. Lin, L. Shen, Z. Ren, W. Wu, Y. Tan, H. Fu, J. Zhang and L. Wu, Enhanced photocatalytic hydrogen production activity via dual modification of MOF and reduced graphene oxide on CdS, *Chem Commun (Camb)*, 2014, **50**, 8533-8535.
8. V. S. Vyas, F. Haase, L. Stegbauer, G. Savasci, F. Podjaski, C. Ochsenfeld and B. V. Lotsch, A tunable azine covalent organic framework platform for visible light-induced hydrogen generation, *Nat Commun*, 2015, **6**, 8508.
9. Z. M. Zhang, T. Zhang, C. Wang, Z. K. Lin, L. S. Long and W. B. Lin, *J. Am. Chem. Soc.*, 2015, **137**, 3197-3200.
10. T. Toyao, M. Saito, S. Dohshi, K. Mochizuki, M. Iwata, H. Higashimura, Y. Horiuchi and M. Matsuoka, Development of a Ru complex-incorporated MOF photocatalyst for hydrogen production under visible-light irradiation, *Chem Commun (Camb)*, 2014, **50**, 6779-6781.
11. Q. Zhang, Y. Wang, Y. Su, Z. Liu, W. Xiao, H. Pang and P. Zhang, CdS-decorated surface-coarsened TiO<sub>2</sub> nanobelts with enhanced visible-light photocatalytic performances, *Journal of Materials Science: Materials in Electronics*, 2020, **31**, 4931-4942.